Microtubular architecture of biodegradable polymer scaffolds

Peter X. Ma,[1–3] Ruiyun Zhang[1]
[1]*Department of Biologic and Materials Sciences, 1011 North University Avenue, Room 2211, University of Michigan, Ann Arbor, Michigan 48109-1078*
[2]*Department of Biomedical Engineering, University of Michigan, Ann Arbor, Michigan*
[3]*Macromolecular Science and Engineering Center, University of Michigan, Ann Arbor, Michigan*

Received 5 October 2000; revised 2 March 2001; accepted 13 March 2001

Abstract: It is a relatively new approach to generate tissues with mammalian cells and scaffolds (temporary synthetic extracellular matrices). Many tissues, such as nerve, muscle, tendon, ligament, blood vessel, bone, and teeth, have tubular or fibrous bundle architectures and anisotropic properties. In this work, we have designed and fabricated highly porous scaffolds from biodegradable polymers with a novel phase-separation technique to generate controllable parallel array of microtubular architecture. Porosity as high as 97% has been achieved. The porosity, diameter of the microtubules, the tubular morphology, and their orientation are controlled by the polymer concentration, solvent system, and temperature gradient. The mechanical properties of these scaffolds are anisotropic. Osteoprogenitor cells are seeded in these three-dimensional scaffolds and cultured *in vitro*. The cell distribution and the neo-tissue organization are guided by the microtubular architecture. The fabrication technique can be applied to a variety of polymers, therefore the degradation rate and cell–matrix interactions can be controlled by the chemical composition of the polymers and the incorporation of bioactive moieties. These microtubular scaffolds may be used to engineer a variety of tissues with anisotropic architecture and properties. © 2001 John Wiley & Sons, Inc. J Biomed Mater Res 56: 469–477, 2001

Key words: scaffold; tube; tubule; matrix; tissue engineering; porous; bone; regeneration

INTRODUCTION

One of the goals of tissue engineering is to create biological alternatives to harvested tissues and organs for transplantation.[1] Scaffolding plays a crucial role in the three-dimensional neo-tissue formation.[2–4] Synthetic biodegradable polymers are attractive candidates for scaffolding fabrication because they do not carry the risk of pathogen transmission and immunorejection, and because they degrade and resorb after fulfilling the scaffolding function, therefore eliminating the long-term inflammation and complications associated with foreign body reactions.[5–8] Each tissue or organ has its characteristic architectural organization, which is closely related to its physiological function. Many organs and tissues have tubular or fibrous bundle architectures. The technology to fabricate single tubular structure at the macro-size scale (a millimeter or larger) such as vascular grafts are available although the development of perfect vascular grafts is still challenging. We report the fabrication of novel biodegradable polymer scaffolds of an organized array of open microtubules with a phase-separation technique. We have demonstrated the control over the microtubule size, porosity, architecture, and mechanical properties with compositional and processing variables. These novel scaffolds possess anisotropic mechanical properties. The mechanical properties along the longitudinal direction of microtubules are significantly better than those along a transverse direction to the axis of the tubules. We have further demonstrated that the microtubular architecture can guide cell seeding, distribution, and new tissue formation *in vitro* in three dimensions.

Correspondence to: P. X. Ma; e-mail: mapx@umich.edu
Contract grant sponsor: DuPont (Young Professor Award)
Contract grant sponsor: The Whitaker Foundation (Biomedical Engineering Research Grant)
Contract grant sponsor: the Center for Biomedical Engineering Research at the University of Michigan (Pilot Grant)

MATERIALS AND METHODS

Scaffold fabrication

Poly(L-lactic acid) (PLLA) and poly(D,L-lactic acid-*co*-glycolic acid) (85/15) (PLGA85/15) with inherent viscosity

of approximately 1.6 (except where indicated differently) and 1.4 were purchased from Boehringer Ingelheim (Ingelheim, Germany). Poly(D,L-lactic acid-*co*-glycolic acid) (75/25) (PLGA75/25) with an inherent viscosity of 0.5–>0.6 was purchased from Medisorb Technologies International (Cincinnati, OH). The PLLA or PLGAs were dissolved in either benzene or dioxane (both from Aldrich Chemical, Milwaukee, WI) to form solutions with desired concentrations. The scaffolds with isotropic pore architecture were fabricated similarly to a procedure previously described for dioxane systems.[9] Briefly, a glass beaker or Teflon vial containing the polymer solution was transferred into a freezer set to a chosen temperature to induce solid-liquid phase separation. For the oriented microtubular scaffolds, the phase separation was performed with a uniaxial temperature gradient. To achieve this directional temperature gradient, the beaker side was wrapped with a layer of thermal insulating material to reduce the heat transfer through the side wall, and the beaker was set on top of a block of metal in a freezer to increase the heat conduction along the longitudinal direction. The phase-separation temperature was −20°C unless indicated differently in the text. The phase-separated polymer/solvent systems were then transferred into a freeze-drying vessel at −5° to −10°C in an ice/salt bath, and was freeze-dried under vacuum (pressure lower than 0.5 mmHg) for 2 weeks. The dried scaffolds were then kept in a desiccator until characterization or usage.

Structure/property characterization

The density and porosity were determined using a method similar to that reported previously.[6] A cube (5 × 5 × 5 mm) was cut out of a scaffold sample. The volume was calculated from accurately measured dimensions, and the mass was measured with an analytical balance. Six specimens of each scaffold were measured to calculate an average density D_f. The porosity ε was calculated from the measured scaffold density D_f and the polymer skeletal density D_p:

$$\varepsilon = \frac{D_p - D_f}{D_p} \tag{1}$$

where the skeletal density of PLLA was determined by:

$$D_p = \frac{1}{\frac{1 - X_c}{D_a} + \frac{X_c}{D_c}} \tag{2}$$

where X_c was the degree of crystallinity determined with differential scanning calorimetry as described elsewhere.[6] For PLLA, D_a = l.248 g/mL (density of amorphous polymer) and D_c = 1.290 g/mL (density of 100% crystalline polymer). The densities of the amorphous copolymers PLGA85/15 and PLGA75/25 were 1.27 and 1.30 g/mL, respectively.

The scaffold architectures were examined with scanning electron microscopy (SEM) (S-3200N; Hitachi, Tokyo, Japan) at 15 kV. The specimens were coated with gold using a sputter coater (Desk-II; Denton Vacuum Inc., Moorestown, NJ).

The diameters of the microtubules were measured from SEM micrographs. More than 40 microtubules were measured to calculate an average diameter. The percentage of ladder-like microtubules in each specimen was calculated also from SEM micrographs. For each scaffold, at least 40 microtubules were examined. The ratio of the number of tubules with ladder-like architecture to the total number of microtubules examined (open tubules + ladder-like tubules) was calculated.

The compressive mechanical properties of the scaffolds were measured with an MTS mechanical tester (Model: Synergie 200; MTS Systems Corporation, Cary, NC). Cubic specimens with a side length of 5 mm were compressed with a crosshead speed of 0.5 mm/min. For samples with anisotropic pore architectures, the load was applied in the direction either parallel to the tubular axis (longitudinal direction) or perpendicular to the tubular axis (transverse direction). The compressive modulus was determined from the initial linear region of the stress-strain curve, and the yield strength was determined from the cross point of the two tangents on the stress-strain curve around the yield point. At least six specimens were tested for each sample, and the averages and standard deviations were graphed. A one-tail Student's t test (assuming unequal variances) was performed to determine the statistical significance ($p < 0.05$).

Tissue culture

The thawed MC3T3-E1 osteoprogenitor cells (clone no. 4, a well characterized cell line that is known to synthesize bone matrix proteins,[10,11] was generously provided by Dr. R. Franceschi at the University of Michigan) were cultured in a supplemented ascorbic acid-free α-MEM (Formula no. 94-5049EL, 10% fetal bovine serum, 50 U/mL penicillin, and 50 μg/mL streptomycin) in a humidified incubator at 37°C with a CO_2/air ratio of 5:95. The medium was changed every other day. The cells of passages 3 or 4 were seeded onto the PLLA scaffolds. The viability of the cells before seeding was higher than 90% determined with the trypan blue exclusion assay.

The porous PLLA disks (with isotropic or anisotropic architectures) with a diameter of 10 mm and a thickness of 1.5 mm were prepared from a 5% polymer solution (in either benzene or dioxane). These scaffolds were assembled on the bottoms of custom-made 12-well Teflon culture plates with a well diameter of 10 mm. The scaffold-containing culture plates were sterilized with ethylene oxide. The sterilized PLLA scaffolds (assembled in the wells) were soaked in ethanol for 30 min, and then exchanged with phosphate buffered saline three times (30 min each). The scaffolds were then washed with a "complete medium" (α-MEM, 10% fetal bovine serum, 50 U/mL penicillin, 50 μg/mL streptomycin, and additional 50 mg/L of L-ascorbic acid) two times (2 h/each). The medium was then decanted and 2 million cells (suspended in 0.5 mL of the complete medium) were seeded on each scaffold. The cell-scaffold constructs were cultured on an orbital shaker (Model 3520; Lab-Line Instruments, Melrose Park, IL) at 75 rpm in the humidified incubator. The medium was changed two times a day (0.5 mL) for 2 days. After the 48-h cell seeding, the cell-scaffold constructs were

removed from the Teflon plates and transferred into 6-well tissue culture plates. The constructs were cultured with the complete medium on the orbital shaker at 75 rpm in the humidified incubator. Four-milliliter medium was used for each construct and the medium was changed every other day. The cell-scaffold constructs were harvested after 4 weeks *in vitro* and fixed in 10% neutral buffered formalin. Paraffin-embedded disk specimens were cut into 5-μm thick cross-sections, and stained with von Kossa's silver nitrate.

RESULTS

Microtubular architecture

The processing parameters, such as temperature gradient, polymer type, solvent type, and the concentration of polymer solution, were studied for their effects on the architectural features of the scaffolds. When a temperature gradient was maintained uniaxially during the thermally induced phase-separation process, the characteristic architecture of an array of parallel microtubules was achieved [Fig. 1(a–e) and (g–i)]. When the temperature gradient was not uniaxial, the pore architecture was randomly oriented [Fig. 1(f)]. At a very low polymer concentration, incomplete tubular architecture (with ribbon- and fiber-like features) with minimum mechanical strength was formed [Fig. 1(a)]. At suitable polymer concentrations, the architecture of an array of parallel open microtubules was achieved [Fig. 1(b,c,e,g). The cross-sections of the microtubules were polygons with 3–7 sides [Fig. 1(e)]. At a very high polymer concentration, the resulting scaffolds had an oriented ladder-like (parallel microtubules with thin partitions) architecture [Fig. 1(d)]. The polymer type (PLLA vs. PLGA: semicrystalline polymer versus amorphous polymer) did not have a significant effect on the formation of the microtubular architecture [Fig. 1(c) vs. (g)]. As the concentration of the polymer solution was decreased, the porosity of the formed scaffolds was increased (Table I). Porosity as high as 97% was achieved with the scaffolds of open microtubular architecture. The porosity of the scaffolds was not significantly affected by the directional temperature gradient (tubular architecture), polymer type, or solvent type used (Table I). Increasing polymer concentration and phase-separation temperature favored ladder-like tubule formation over the open tubular architecture (Table II). The diameter of the tubules decreased with increasing polymer concentration in the low concentration range, but leveled off above 5% (Table III). The diameter of the tubules increased with phase-separation temperature (Table III). The polymer type and molecular weight (viscosity) did not show significant effect on the diameter of the tubules (Table III).

The solvent type showed a clear effect on the microarchitecture of the polymer scaffolds: benzene favored the open tubular structure formation whereas dioxane favored the ladder-like structure formation [Fig. 1(c,e) vs. (h,i)]. This was likely because of the nature of the solid-liquid phase separation, i.e., the crystallization of the solvent to control the architecture formation. The pore geometry was determined by the crystallized solvent, which was subsequently sublimated to form the pores.[9] A possible reason for benzene and dioxane to result in different pore architectures (open tubular vs. ladder-like) might be the difference of the melting points of these two solvents. Because dioxane has a higher melting point (T_m = 11.8°C) than benzene (T_m = 5.5°C), the polymer/dioxane solution has a higher degree of super-cooling than that of the polymer/benzene solution at the same phase-separation temperature (−20°C), which might have resulted in different solvent crystallization kinetics (faster nucleation and slower growth of the dioxane crystals in the polymer/dioxane system) and therefore the different pore architectures of the porous materials. Another possible reason might be that the different polymer-solvent interactions led to different viscosities of the systems, which affected the phase-separation kinetics. The third possible reason might be that the different crystal structures of the two solvents contributed to the differences in the tubular architecture. These factors could have individually or conjointly resulted in the architectural differences of the scaffolds from the two different solvents.

Mechanical properties

The architectural anisotropy led to anisotropic mechanical properties of the microtubular scaffolds (Fig. 2). Both the compressive modulus and the yield strength of a scaffold with microtubular architecture were significantly greater in the longitudinal direction than in a transverse direction ($p < 0.05$ for all samples). The scaffolds of isotropic architecture showed isotropic mechanical properties, which fell in between those of the longitudinal and transverse directions of the oriented microtubular scaffolds of the same polymer and polymer concentration (Fig. 2). Both the compressive modulus and the compressive yield strength increased with polymer concentration for both the isotropic and anisotropic scaffolds as expected [Fig. 2(a,d)]. With the same polymer concentration used, the PLLA scaffolds had significantly higher modulus and yield strength than the PLGA copolymer scaffolds [Fig. 2(b,e)] in both longitudinal and transverse directions likely because of the crystallinity and higher molecular weight (inherent viscosity) of the PLLA used. The two different oriented architectures (open micro-

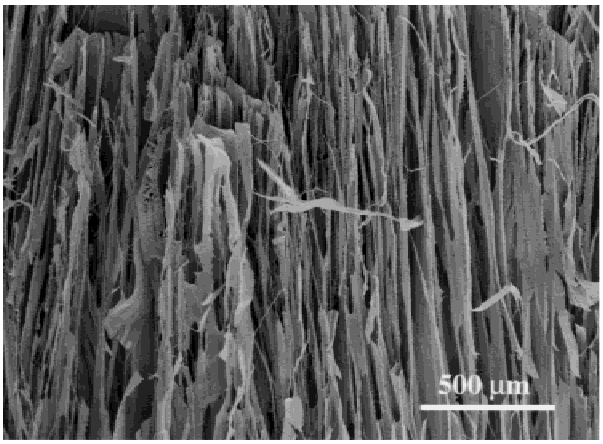

(a)

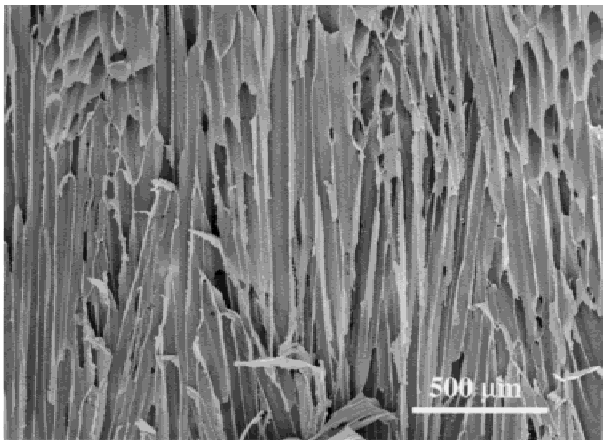

(b)

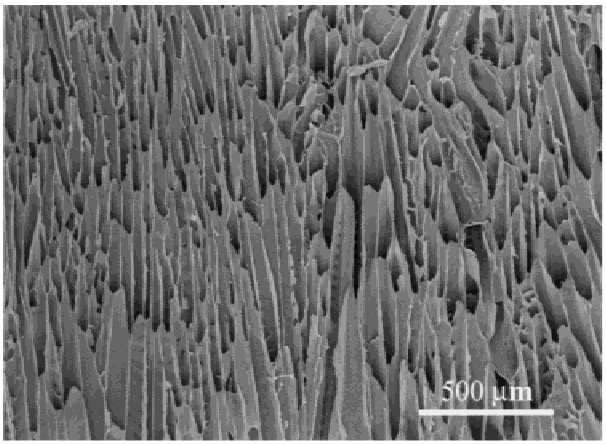

(c)

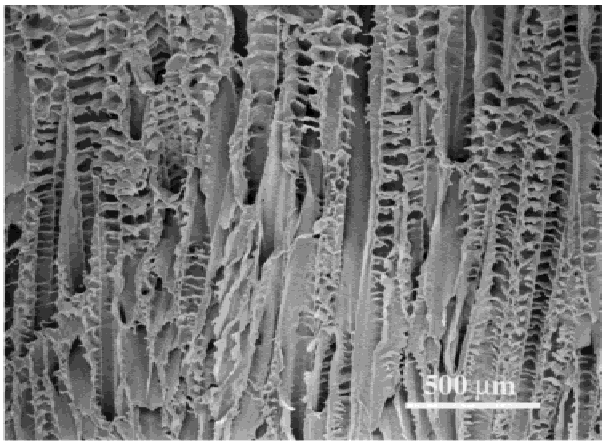

(d)

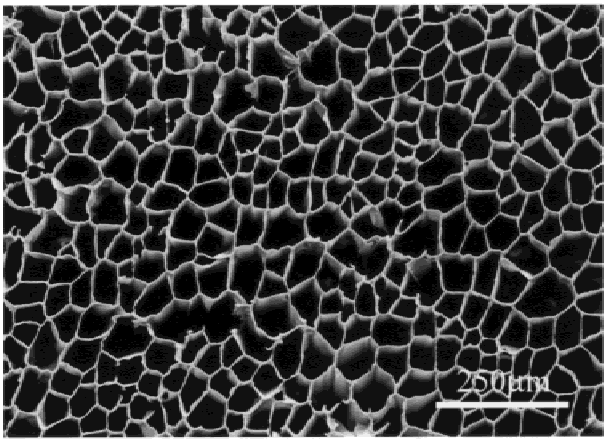

(e)

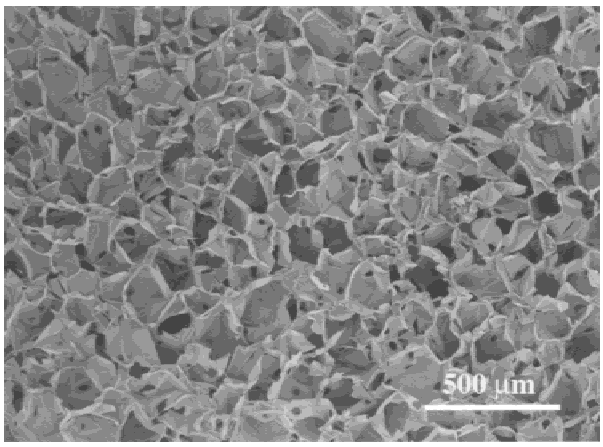

(f)

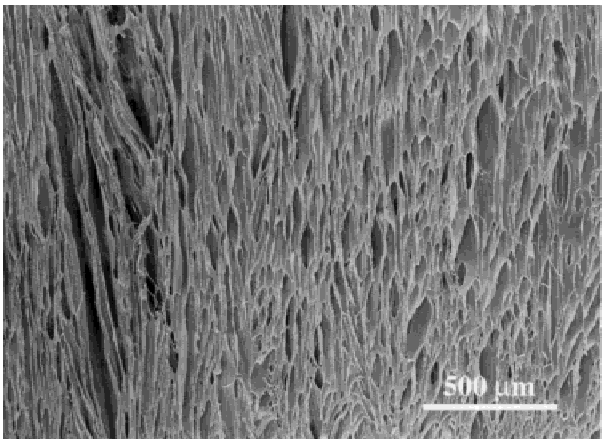

(g)

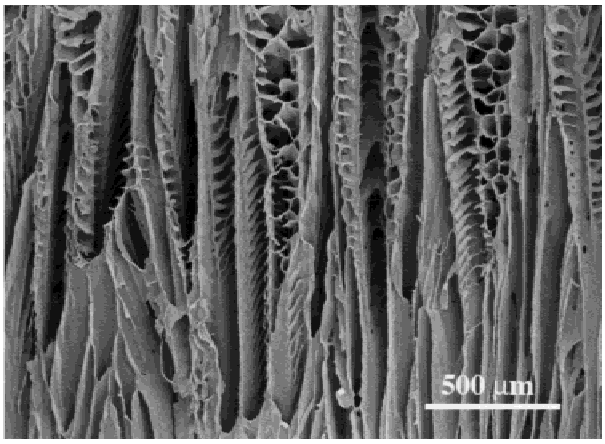

(h)

tubular and ladder-like) of the scaffolds resulting from the two different solvents used (benzene and dioxane) also led to differences in mechanical properties. The modulus of the PLLA scaffolds of parallel open microtubular architecture (benzene as the solvent) was slightly higher than that of the scaffolds with a ladder-like architecture (dioxane as the solvent) in the longitudinal direction [Fig. 2(c)], though not statistically significant, $p = 0.39$). The modulus of the scaffold with parallel open microtubular architecture was significantly lower ($p = 0.029$) than that of the scaffold with ladder-like architecture in a transverse direction [Fig. 2(c)]. Similarly, the yield strength of the scaffold with the open tubular architecture was significantly higher ($p = 6 \times 10^{-5}$) than that of the scaffold with ladder-like architecture in the longitudinal direction whereas the yield strength of the scaffold with open tubular architecture was significantly lower ($p = 0.006$) than that of the scaffold with ladder-like architecture in a transverse direction [Fig. 2(f)]. The better mechanical properties of the scaffolds with ladder-like structure in the transverse direction were likely due to the contribution of partitions perpendicular to the tubule axis (parallel to the transverse direction). The lower mechanical properties in the longitudinal direction of the scaffold with ladder-like architecture were likely due to the reduced total cross-sectional area of the tubular walls because a certain amount of polymer was taken by the partitions.

In vitro tissue formation

To test how cells and new tissue organization respond to the three-dimensional architecture of the scaffolds, MC3T3-El cells were seeded on the scaffolds of the same polymer (PLLA) and of the same porosity but with different three-dimensional architectural features (Fig. 3). The cell distribution followed the architectural features. After 4 weeks of *in vitro* culture, the cells in the open microtubular scaffolds were organized along the oriented tubular directions to form oriented neo tissue [Fig. 3(a)], which was somewhat similar to dentin or long bone in tissue architecture. The cells and the neo tissue in the scaffold of the ladder-like structure were organized along the ladder-like architecture [Fig. 3(b)]. The cells and the neo tissue in the scaffold of random orientation were randomly distributed [Fig. 3(c)]. Repeated histological analyses suggested that the neo-tissue formation was more enhanced in the scaffolds of tubular architectures than in those of random pore architecture, which could have resulted from the improved mass transport or/and cell–cell interactions.

DISCUSSION

It is well recognized that scaffolding plays a critical role in tissue engineering. There are active research activities in studying the effects of patterning material surfaces on cell organization in two-dimensional models.[12–14] Research in this area has led to significant new understandings in cell–matrix interactions. However, in the body, cells are surrounded by cells and the extracellular matrix in a three-dimensional environment. There is little understanding of cell–cell interactions and cell–matrix interactions in these three-dimensional systems. This work has demonstrated that cells pattern and organize themselves following the architectural clues in the synthetic biodegradable polymer scaffolds in three dimensions.

Many tissues, such as nerve, muscle, tendon, ligament, vasculature, bone, and teeth, have organized fibrillar or tubular architectures. In this work, we have successfully created biodegradable polymer scaffolds with the architecture of a parallel array of open microtubules, and have demonstrated how to control the

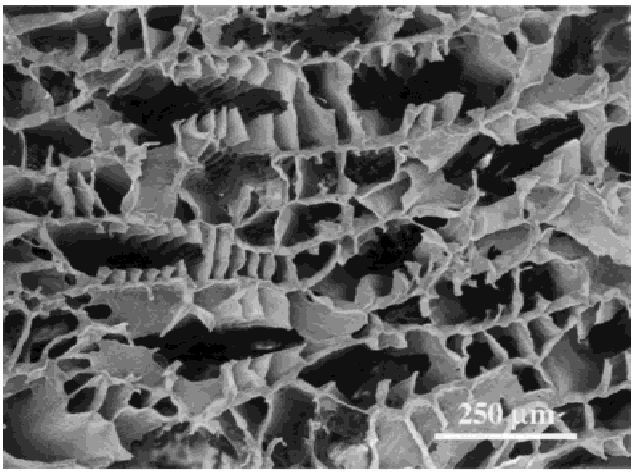

Figure 1. SEM micrographs of porous PLLA and PLGA scaffolds prepared with their solutions in benzene and dioxane using a phase-separation technique. (a) 1.0% (wt/v) PLLA/benzene, uniaxial temperature gradient, longitudinal section; (b) 2.5% (wt/v) PLLA/benzene, uniaxial temperature gradient, longitudinal section; (c) 5.0% (wt/v) PLLA/benzene, uniaxial temperature gradient, longitudinal section; (d) 10.0% (wt/v) PLLA/benzene, uniaxial temperature gradient, longitudinal section; (e) 5.0% (wt/v) PLLA/benzene, uniaxial temperature gradient, cross-section; (f) 5.0% (wt/v) PLLA/benzene, nondirectional temperature gradient; (g) 5.0% (wt/v) PLGA(85/15)/benzene, uniaxial temperature gradient, longitudinal section; (h) 5.0% (wt/v) PLLA/dioxane, uniaxial temperature gradient, longitudinal section; (i) 5.0% (wt/v) PLLA/dioxane, uniaxial temperature gradient, cross-section.

TABLE I
Densities and Porosities of the PLLA and PLGA Scaffolds

Polymer	Solvent	Concentration (wt/v %)	Phase-Separation Temperature (°C)	Pore Structure	Density (g/cm^3)	Porosity (%)
PLLA	Benzene	2.5	−20	Tubular	0.038	97.0
PLLA	Benzene	2.5	−20	Random	0.037	97.1
PLLA	Benzene	5.0	−20	Tubular	0.078	93.8
PLLA	Benzene	5.0	−20	Random	0.074	94.1
PLLA	Benzene	7.5	−20	Tubular	0.105	91.7
PLLA	Benzene	7.5	−20	Random	0.110	91.3
PLLA	Benzene	10.0	−20	Tubular	0.140	88.9
PLLA	Benzene	10.0	−20	Random	0.141	88.8
PLLA	Dioxane	5.0	−20	Tubular	0.084	93.3
PLLA	Dioxane	5.0	−20	Random	0.084	93.4
PLGA (85/15)	Benzene	5.0	−20	Tubular	0.079	93.7
PLGA (85/15)	Benzene	5.0	−20	Random	0.074	94.1
PLGA (75/25)	Benzene	5.0	−20	Tubular	0.086	93.5
PLGA (75/25)	Benzene	5.0	−20	Random	0.073	94.2

architectural parameters such as porosity, diameter of the tubules, and the formation of partitions in the tubular architecture with the processing parameters such as polymer concentration, solvent type, and temperature gradient. As demonstrated with the osteoblastic cells in this work, other cell types also are likely to follow the architectural clues of the scaffolds to form fibrous bundle or microtubular architecture in these novel scaffolds *in vitro* and *in vivo*.

The fabrication technology described in this work is versatile and has the general applicability to other polymers. It has been demonstrated that the solvent type plays a more important role than the polymer type in determining the micropore architecture. The biodegradability can be controlled by designing or selecting the right chemical structure of the polymer to obtain the desired degradation rate without significantly affecting the scaffolding architecture if the solvent type and the temperature gradient are maintained the same. Similarly, the surface properties of the scaffolds such as hydrophilicity, charge type, charge density, biological functionality may also be manipulated by designing or selecting the right chemical structure and functionality of the polymers.

TABLE II
Percentage of Microtubules with Ladder-Like Architecture Changes with PLLA/Benzene Concentration and Phase-Separation Temperature

Polymer	Concentration (wt/v %)	Phase-Separation Temperature (°C)	Percentage of Ladder-Like Tubules
PLLA	5.0	−20	13.0
PLLA	7.5	−20	40.4
PLLA	10.0	−20	48.5
PLLA	12.5	−20	54.9
PLLA	15.0	−20	63.5
PLLA	5.0	Liquid N_2	0
PLLA	5.0	−10	30.5

The internal surfaces of the porous scaffolds may also be modified post-scaffold fabrication. The technology may also be used to fabricate scaffolds of polymer blends, mixtures, and composites with the desired microtubular architectures. Therefore, the technology can be used to fabricate matrices with both cell delivery and bioactive molecule delivery capabilities. The new microtubular architecture may serve as superior scaffolds for the engineering of a variety of tissues with fibrillar or tubular architectures.

To guide peripheral nerve repair, for example, tubes made of natural and synthetic materials have been used.[15–18] However, a large hollow tube is not as effective as tubes filled with oriented fibrous[19] or tubular[20] materials. The new fabrication technology developed in this work can create the parallel multi-tubule structure in a one-step phase-separation process. The polymers are biodegradable and biocompatible. The

TABLE III
Average Diameter of Microtubule Changes with the Polymer Concentration and Phase-Separation Temperature

Polymer	Inherent Viscosity (dL/g)	Concentration (wt/v %)	Phase-Separation Temperature (°C)	Average Diameter (μm)
PLLA	1.6	2.5	−20	96.3
PLLA	1.6	5.0	−20	61.5
PLLA	1.6	7.5	−20	61.2
PLLA	1.6	10.0	−20	54.9
PLLA	1.6	12.5	−20	54.7
PLLA	1.6	15.0	−20	59.1
PLLA	1.6	5.0	Liquid N_2	28.2
PLLA	1.6	5.0	−10	71.5
PLLA	1.6	5.0	0	113.4
PLGA (85/15)	1.4	5.0	−20	54.1
PLLA[a]	1.0[a]	5.0	−20	57.9

[a]This PLLA has a different inherent viscosity than that of the PLLA used for other scaffolds.

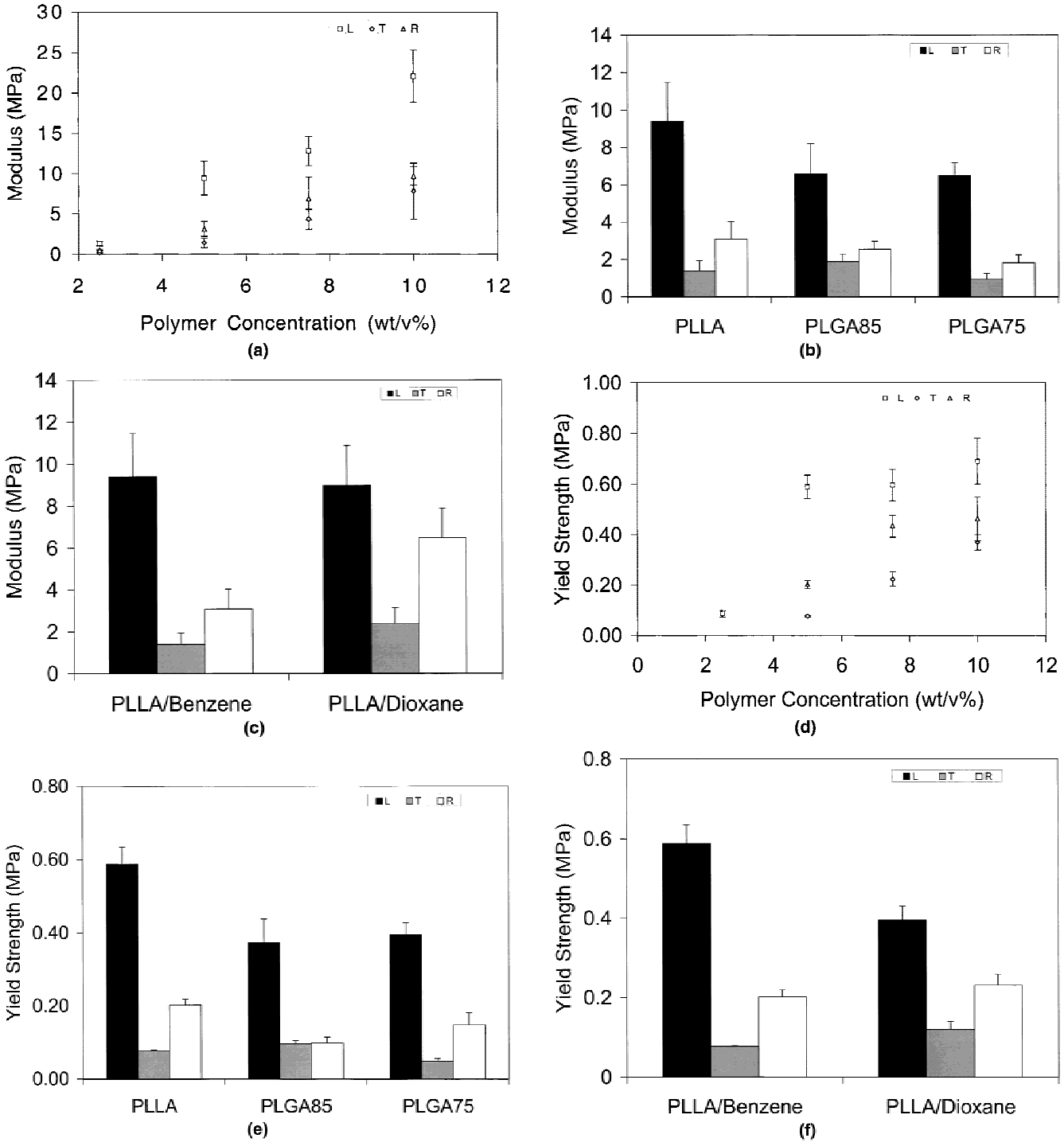

Figure 2. Compressive mechanical properties of porous PLLA and PLGA scaffolds prepared with their solutions in benzene and dioxane using a phase-separation technique. (a) Modulus of scaffolds with tubular or random pore architecture prepared from PLLA/benzene solutions of varying concentrations; (b) modulus of scaffolds prepared from 5.0% (wt/v) PLLA/benzene or PLGA/benzene solution with tubular or random pore architecture; (c) modulus of scaffolds prepared from 5.0% (wt/v) PLLA/benzene or PLLA/dioxane solution with tubular or random pore architecture; (d) yield strength of scaffolds with tubular or random pore architecture prepared from PLLA/benzene solutions of varying concentrations; (e) yield strength of scaffolds prepared from 5.0% (wt/v) PLLA/benzene or PLGA/benzene solution with tubular or random pore architecture; (f) yield strength of scaffolds prepared from 5.0% (wt/v) PLLA/benzene or PLLA/dioxane solution with tubular or random pore architecture. Notes: L, loading direction is parallel to the longitudinal direction; T, loading direction is along a transverse direction; R, scaffolds with random pore architecture.

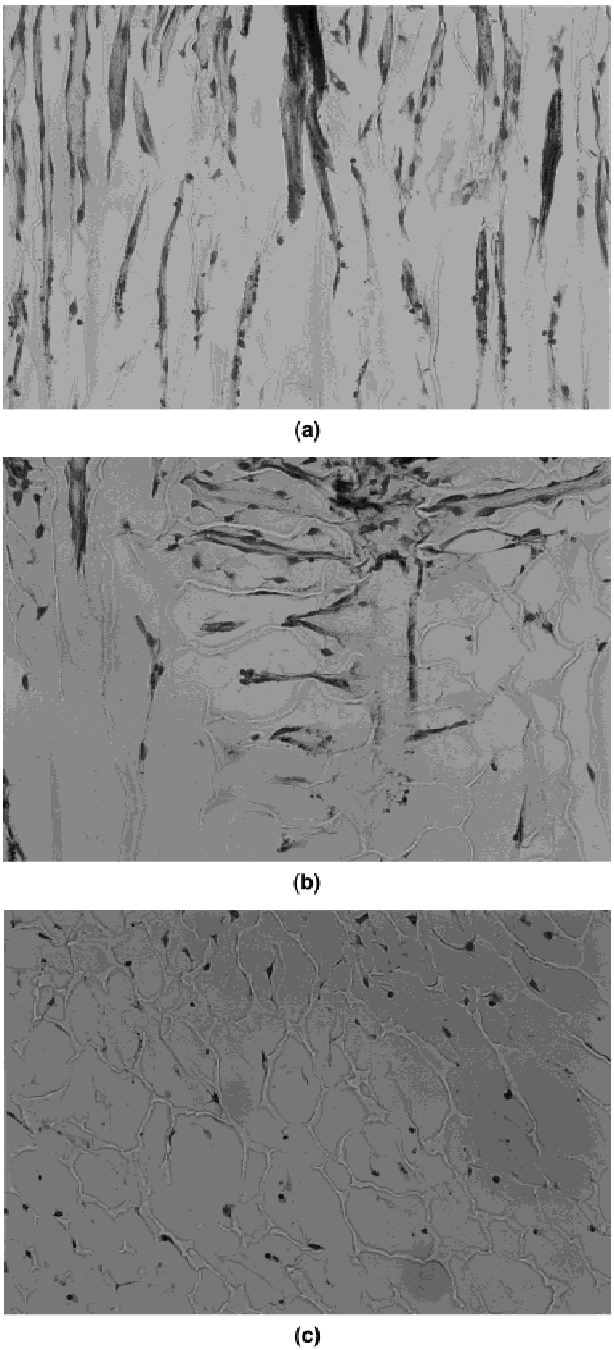

Figure 3. Cell (MC3T3-E1 clone no.4, see Materials and Methods)–scaffold constructs stained with von Kossa's silver nitrate after being cultured for 4 weeks. (a) PLLA scaffold with open microtubular architecture prepared from 5.0% (wt/v) PLLA/benzene solution; (b) PLLA scaffold with ladder-like microtubular architecture prepared from 5.0% (wt/v) PLLA/dioxane solution; (c) PLLA scaffold with open random pore architecture prepared from a 5.0% (wt/v) PLLA/benzene solution.

porosity and pore size can be controlled. The fabrication technology has the potential to incorporate bioactive factors, and the scaffold can be designed for the growth of nerve-supporting cells such as Schwann cells. Therefore, the scaffolds can be tailored into synthetic conduits for nerve repair.

Many tissues with anisotropic structures such as tendon, ligament, muscle, bone, and dentin also have anisotropic mechanical properties. We have demonstrated the anisotropic mechanical properties of these microtubular scaffolds, which might match the mechanical properties better to those of the tissues to be replaced or repaired.

In summary, with the capability of controlling a variety of chemical and architectural features of the open microtubular scaffolds, the new scaffolding technology can be used to generate tailor-designed scaffolds for the engineering of a variety of oriented tubular or fibrillar tissues. The technology may also be used to fabricate novel porous materials (from degradable or nondegradable polymers) for other biomedical and industrial applications such as wound dressing, controlled release, substrate for biological and chemical reactions, extracorporal devices (e.g., artificial kidney), filtration membrane, insulating, packaging, and mechanically damping materials.

References

1. Langer R, Vacanti JP. Tissue engineering. Science 1993; 260(5110):920–926.
2. Hubbell JA. Biomaterials in tissue engineering. Biotechnology 1995;13(6):565–576.
3. Zhang R, Ma PX. Synthetic nano-fibrillar extracellular matrices with predesigned macroporous architectures. J Biomed Mater Res 2000;52(2):430–438.
4. Ma PX, Choi J. Biodegradable polymer scaffolds with well-defined interconnected spherical pore network. Tissue Eng 2001;7(1):23–33.
5. Lu L, Garcia CA, Mikos AG. *In vitro* degradation of thin poly(DL-lactic-*co*-glycolic acid) films. J Biomed Mater Res 1999;46(2):236–244.
6. Ma PX, Zhang R. Synthetic nano-scale fibrous extracellular matrix. J Biomed Mater Res 1999;46(1):60–72.
7. Kim SS, Utsunomiya H, Koski JA, Wu BM, Cima MJ, Sohn J, Mukai K, Griffith LG, Vacanti JP. Survival and function of hepatocytes on a novel three-dimensional synthetic biodegradable polymer scaffold with an intrinsic network of channels. Ann Surg 1998;228(1):8–13.
8. Ma PX, Schloo B, Mooney D, Langer R. Development of biomechanical properties and morphogenesis of *in vitro* tissue engineered cartilage. J Biomed Mater Res 1995;29(12):1587–1595.
9. Zhang R, Ma PX. Poly(alpha-hydroxyl acids)/hydroxyapatite porous composites for bone-tissue engineering. I. Preparation and morphology. J Biomed Mater Res 1999;44(4):446–455.
10. Xiao G, Cui Y, Ducy P, Karsenty G, Franceschi RT. Ascorbic acid-dependent activation of the osteocalcin promoter in MC3T3-E1 preosteoblasts: Requirement for collagen matrix synthesis and the presence of an intact OSE2 sequence. Mol Endocrinol 1997;11(8):1103–1113.
11. Ma PX, Zhang R, Xiao G, Franceschi R. Engineering new bone tissue *in vitro* on highly porous poly(alpha-hydroxyl acids)/hydroxyapatite composite scaffolds. J Biomed Mater Res 2001;54(2):284–293.
12. Kam L, Shain W, Turner JN, Bizios R. Correlation of astroglial cell function on micro-patterned surfaces with specific geometric parameters. Biomaterials 1999;20(23-24):2343–2350.
13. Thomas CH, Lhoest JB, Castner DG, McFarland CD, Healy KE.

Surfaces designed to control the projected area and shape of individual cells. J Biomech Eng 1999;121(1):40–48.
14. Kane RS, Takayama S, Ostuni E, Ingber DE, Whitesides GM. Patterning proteins and cells using soft lithography. Biomaterials 1999;20(23-24):2363–2376.
15. Schmidt CE, Shastri VR, Vacanti JP, Langer R. Stimulation of neurite outgrowth using an electrically conducting polymer. Proc Natl Acad Sci USA 1997;94(17):8948–8953.
16. Hudson TW, Evans GR, Schmidt CE. Engineering strategies for peripheral nerve repair. Clin Plast Surg 1999;26(4):617–628, ix.
17. Yannas IV. Applications of ECM analogs in surgery. J Cell Biochem 1994;56(2):188–191.
18. Bamber NI, Li H, Aebischer P, Xu XM. Fetal spinal cord tissue in mini-guidance channels promotes longitudinal axonal growth after grafting into hemisected adult rat spinal cords. Neural Plast 1999;6(4):103–121.
19. Ceballos D, Navarro X, Dubey N, Wendelschafer-Crabb G, Kennedy WR, Tranquillo RT. Magnetically aligned collagen gel filling a collagen nerve guide improves peripheral nerve regeneration. Exp Neurol 1999;158(2):290–300.
20. Hadlock T, Elisseeff J, Langer R, Vacanti J, Cheney M. A tissue-engineered conduit for peripheral nerve repair. Arch Otolaryngol Head Neck Surg 1998;124(10):1081–1086.